2012

Chemotaxis of Drosophila Glia with Controlled Microenvironments

Cade Beck
CUNY City College

Chemotaxis of Drosophila Glia within Controlled Microenvironments

Thesis

Submitted in partial fulfillment of the requirement for the degree

Master of Science in Biomedical Engineering

at

The City College of New York

of the

City University of New York

By Cade Beck

May 2012

Approved:

Professor Maribel Vazquez, Thesis Advisor	Professor John Tarbell, Chairman Department of Biomedical Engineering

TABLE OF CONTENTS

ABSTRACT

FGF signaling has been shown to be important for many aspects of Drosophila development such as mesoderm spreading and tracheal branching. In the developing Drosophila eye, retinal basal glia migrate through the optic stock into the eye imaginal disc. Blocking FGFR prevented this migration, so it was believed that an FGF molecule was the diffusible signal directing it. This study utilized the Gal4-UAS system to drive GFP expression in glia. These cells were then dissociated and cultured in a microfluidic device capable of generating gradients as well as 96 well plates for uniform FGF-8 concentrations. The purpose was to see if FGF-8 was a chemoattractant for glia, as suggested by earlier in vivo work. That will further our understanding of the molecular mechanisms driving glia migration, which could lead to treatments for disorders caused by improper migration.

Cells were imaged for 48 hours and their trajectories plotted. Experiments were repeated for three initial concentrations of FGF-8: 1 ng/mL, 10 ng/mL, and 100 ng/mL; and two groups of cells: pure glia populations isolated via FACS ("sorted"), and a mixed population of neurons and glia obtained directly from dissociated brains ("unsorted"). FGF-8 did in fact turn out to stimulate motility in the glia but only with unsorted cells, suggesting a complex signaling network that relies on multiple interdependent ligands. In the wells, unsorted cells increased motility and distance traveled significantly for all concentrations, with peak results at 10 ng/mL. In the microchannel, cells migrated toward the gradient only for 10 and 100 ng/mL. Results peaked at a concentration of 1-10 ng/mL and gradient of 10^{-3} -10^{-2} ng/(mL*mm).

In addition, the diffusivity of FGF-8 was calculated for data analysis. While most frequently used for chemotaxis assays, microfluidic gradient generators are capable of measuring diffusion coefficients of fluorescent molecules as well. Other methods of measuring diffusion

coefficients, such as FRAP and FCS require expensive equipment, sophisticated mathematical models, and have a limited range of molecular weights that will give accurate results. Our study used the μLane system to calculate the diffusivity of 20 kDa FITC-dextran by solving Fick's law of diffusion and curve fitting with measured intensity values. We report a diffusivity of 6.8 +/- .3 $*10^{-7}$ cm^2/s for free solution and an effective diffusivity of 6.1 +/- .2$*10^{-7}$ cm^2/s in a Laminin matrix. These results could easily be repeated for different molecular weights of dextran, and provide good estimates of diffusion coefficients for molecules of similar molecular weight which are not fluorescent.

CHAPTER 1: Background

1.1 Migration of glia in Drosophila

Traditionally overlooked, glia play a crucial role in nearly every aspect of the nervous system. Glia control neuronal differentiation, provide guidance cues for developing axons, wrap and insulate neurons, and provide trophic factors for their continued survival[1]. They also form the blood brain barrier as well as regulate ion and neurotransmitter levels[2]. In *Drosophila*, there are three major classes of glia: surface, cortex, and neurophile[3]. As the names suggest, they are classified based on location rather than function. These classes can also be subdivided into several more groups. There is actually somewhat of a debate over nomenclature, as no clear criteria exist to definitively categorize these cells.

Glia are highly motile cells. Most start as neuroglioblasts and then migrate to their final destination[4] . For example, during embryogenesis two sets of glia associated with the ventral nerve cord, the midline glia and the longitudinal glia, migrate outward on nerve tracts. The number of glia is reduced and migration is halted by ablation of the neurons, indicating neurons are required as a substrate for migration[5]. A similar process happens in the peripheral nervous system. During wing formation, glia migrate along sensory axons[6]. In the zebrafish peripheral nervous system, glia associate with pioneer axons. When axons are misrouted, then the glia follow. If the axons are blocked, glia halt their migration[7].

The Drosophila visual system is comprised of approximately 750 ommatidia, each containing 8 photoreceptor neurons or "R-cells". These cells originate in the eye imaginal disc, and then extend axons through the optic stalk and into the optic lobe[8] (see figure 1). R1-R6 terminates in the lamina, while R7 and R8 terminate deeper in the optic lobe in a region called

the medulla. R-cells axons depend on glia for path finding and also to innervation of the lamina. The visual system contains two types of glia: lamina and subretinal.

Lamina glia migrate to the lamina along scaffold axons. These axons extend from the optic lobe toward photoreceptor axons. The photoreceptors trigger the growth of these scaffolds. When the scaffolds are eliminated, migration doesn't take place. In addition, incorrectly positioned axon scaffolds guide glia to improper locations. Neurons rely on glia just as much, but for trophic signals rather than directional cues. When glia are missing, neurons commit apoptosis[9]. This is more evidence of the interdependence of neurons and glia.

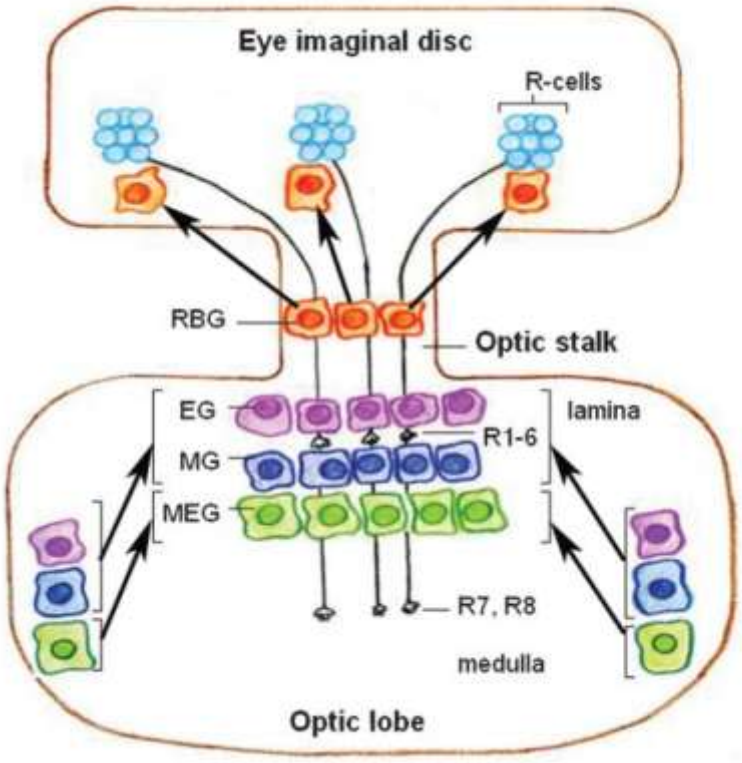

Figure 1: Illustration of glial cell migration in the developing Drosophila visual system. Three ommatidia (light blue) are illustrated in the eye imaginal disc. Photoreceptor (R-Cell) axons extend from the ommatidia toward the optic lobe. Retinal basal glial cells (RBG) migrate along R-Cell axons in an anterior direction from the optic stalk. Lamina glia (EG, MG, MEG) migrate along axon scaffolds toward the lamina. ***Adapted from 12***

Subretinal glia cells, or retinal basal glia (RBG), follow the opposite path of R-cells. They originate in the in the optic stalk and then migrate through the stalk into the eye imaginal disc. This migration is dependent on the presence of R-cells, because in eyes absent and sine oculis - mutants that lack R-cells – RBG failed to migrate. Conversely, overexpression of photoreceptors increased the number of glia that migrated[10]. Because of this, it was proposed that RBG required R-cell axons as a substrate for migration. That seemed reasonable, given the ample evidence of this requirement in so many other contexts. However, a later experiment revealed that is not the case[11]. Mutants were generated that contained R-cells, but had short axons did not descend into the optic stalk. Migration was observed to still occur, disproving the hypothesis that axons are required for migration. In addition, ectopically expressed photoreceptors were capable of attracting glia[11]. Given the evidence, the author suggested two mechanisms for migration: a diffusible chemoattractant, or a contact mechanism where glial filopodia extend toward the axons which then stabilize them and allow them to enter. Given the necessary distance is several times larger than the average glia cell diameter, the second option seems unlikely.

Assuming the chemoattractant model is correct, what then is the chemical signaling molecule that causes migration to take place? Molecules that influence migration in *Drosophila* are incompletely characterized and poorly understood. However, an incomplete list of important ones does exist. These include epidermal growth factor receptor (EGFR), Fibroblast growth factor receptor (FGFR), Roundabout (Robo), Notch, Hedgehog (Hh), Decapentaplegic (Dpp), Gligamesh (Gish) and Fear-of-intimacy (Foi)[12]. Additionally, Loco and Rap/Fzr have been shown to influence the number of glia[13]. Given the number of factors, their interdependence, and their context dependent functions, describing the entire role of each one remains a challenge.

Drosophila has two FGF receptors: Breathless and heartless. Breathless was first described when it was knocked out and tracheal cells failed to migrate, hence the name[14]. Heartless is responsible for the differentiation of mesoderm cells into heart and somatic muscles. It is also responsible for ensheathment of longitudinal axons[15]. While there are only two receptors, there are three ligands that activate them. Branchless (bnl) was shown to induce tracheal branching when it was first discovered, and it binds to the breathless receptor[16]. Pyramus (Pyr) and thisbe (ths) activate the heartless receptor, and are required for mesoderm migration[17]. Later it was discovered that they are not interchangeable, even though they activate the same receptor. During gastrulation, they both support mesoderm spreading, but pyr has a longer range. Additionally, ths- mutants spread abnormally, but did not fail as pyr- mutants[18]. These differences could be accounted for by differential binding affinities for FGFR and/or different diffusion ranges.

Recent work investigated the role of pyr and ths specifically in the drosophila visual system, rather than embryos. Knocking out the htl receptor resulted in 40% reduction of glia, impaired migration, and lack of differentiation[19]. That is evidence that those ligands could be the "unknown" diffusible signal identified earlier. Overexpression resulted in an 8-fold increase in glia number, but interestingly, impaired migration as well. Pyr is expressed in the eye disc, while ths is expressed only in photoreceptor neurons. Initially, pyr controls division and migration, then ths induces differentiation and axonal wrapping[19]. All of that is further evidence that pyr and ths are not interchangeable, and have different biological functions.

FGFs in Drosophila are much larger than their mammalian counterparts. Pyr is 87 kD, and Ths is 82.2 kD. In contrast, FGF-8 is 22.5 kD. At first this may seem surprising, however, the form that Drosophila Schneider cells (S2) secrete is actually about 30 kD[20]. That indicates

that pyr and ths are cleaved intracellularly before being secreted. The FGF domain is retained, and this alone is necessary for function.

1.2 Microfluidic devices and Chemotaxis

Microfluidics has been a research area for decades, but only in the last ten years has it been amenable to simple and inexpensive bench top applications. That is due to replacing silicon with poly dimethylsiloxane (PDMS) as a building material. Silicon was originally used because the technology for fabrication was already available and highly developed in the semiconductor industry. Silicon fabrication is, however, ill suited for use in regular laboratories. It requires expensive equipment as well as clean rooms[21]. PDMS, in contrast, is both cheap and easy to use.

Use of PDMS in microfluidics was developed and popularized by Professor Whitesides, beginning with his seminal paper "Fabrication of Microfluidic Systems in Poly (dimethylsiloxane)"[22]. PDMS is a cross linked polymer with two components: a base and a curing agent. The base has vinyl groups and the curing agent is silicon hydride. These are mixed together in a 10:1 ratio of base to curing agent, and baked at 70 C for 1 hour. The mixing together with the heat forms cross links and the sticky, gooey mixtures hardens into an elastomeric solid.

Because it starts out as a viscous liquid which then hardens, PDMS can be poured into molds to create a wide variety of shapes for many different applications[23]. Molding PDMS is manner is called soft lithography. First, a master is created in the desired shape. This is done primarily via photolithography, but more permanent masters can be micromachined from aluminum as well. Next, the PDMS is poured over the mold, cured, and removed. The final step is bonding. PDMS can be bonded to either itself or glass. This is done by exposing both the

PDMS and glass surfaces to air plasma with an ozone gun. The plasma generates SiOH groups by the oxidation of methyl groups, which then bond to each other. Bonding works best on clean, dry, and flat surfaces. It is also chemically irreversible, although the bond can be broken if enough mechanical force is applied.

Physical, mechanical, and chemical properties of PDMS make it an ideal material for biological applications. With the exception of the plasma oxidation described above, it is chemically inert. It is also biocompatible, nontoxic, and gas permeable, creating a microenvironment where cells can thrive[24]. Lastly, it is transparent, making it suitable for microscopic imaging. Because of its desirable properties, PDMS was quickly adopted to make microfluidic devices capable of generating concentration gradients for use in chemotaxis experiments[25].

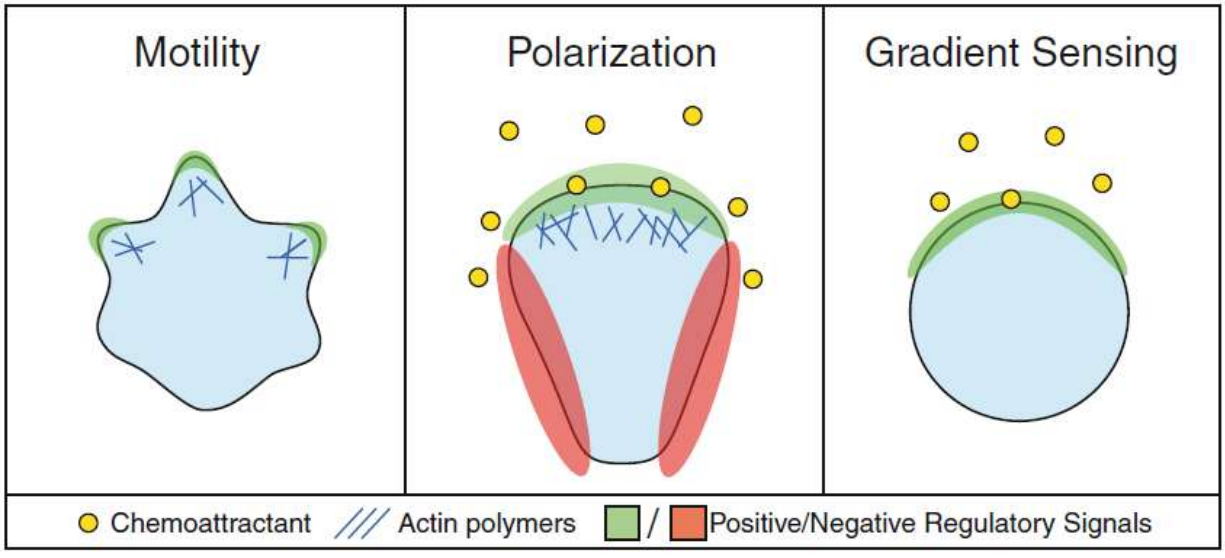

Figure 2: Cellular events involved in chemotaxis. Cell motility is driven by the biased, actin-mediated extension of pseudopod-like extensions at one end of the cell. Some cells are capable of coordinating intracellular and extracellular signaling to promote cell polarization and establish persistent leading and trailing edges. Furthermore, even while immobile, some cells can detect and amplify external chemoattractant gradients, a process termed gradient sensing. ***Adapted from 28***

Chemotaxis is the guided migration of cells toward increasing gradients of chemoattractants. This is the driving force behind the coordinated cellular movement that occurs during embryogenesis, wound healing, and cancer metastasis[26]. Clearly, identifying the specific function of each chemoattractant as well as characterising the relevant concentrations and gradients that maximize cellular response is an important field of study in biomedical research.

Traditionally, Boyden assays have been used in migration experiments[27]. They consist of a porous membrane which sits in a solution of the desired chemoattractant. A layer of cells is plated on top of the membrane, and they allowed to migrate through the pores toward the chemoattractant. At the end of the experiment, the number of cells migrated are counted. The problem with Boyden chambers is that gradients are nonlinear, transient, and difficult to characterize. A researcher is only able to choose an initial concentration, and then sit back until the experiment is over. Cells cannot be imaged in real time, severely limiting scope of what Boyden assays can accomplish. In contrast, microfabricated gradient generators can create well defined and characterized gradients. Because PDMS is optically transparent, cells can also be monitored in real time throughout the course of the experiment.

REFERENCES

1. Thomas JB, Axon guidance: crossing the midline Curr. Biol., 8 (1998), 102–104

2. Auld VJ, Parker RJ. Roles of glia in the Drosophila nervous system. *Seminars in Cell & Developmental Biology* 17 (2006) 66–77

3. Hartenstein V. Morphological diversity and development of glia in Drosophila. *Glia.* 2011 59(9):1237-52

4. V Hartenstein, C Nassif, A Lekven Embryonic development of the Drosophila brain. II. Pattern of glial cells J. Comp. Neurol., 402 (1998), pp. 32–47

5. Kinrade E., Brates T., Tear G. and Hidalgo A. (2001) Roundabout signaling, cell contact and trophic support confine longitudinal glia and axons in the Drosophila CNS. Development 128, 207–216.

6. Giangrande A. Glia in the fly wing are clonally related to epithelial cells and use the nerve as a pathway for migration. Development 1994;120:523–34.

7. Gilmour DT, Maischein HM, Nüsslein-Volhard C. Migration and function of a glial subtype in the vertebrate peripheral nervous system. Neuron. 2002 May 16;34(4):577-88.

8. Clandinin T.R. and Zipursky S.L. (2002) Making connections in the fly visual system. Neuron 35, 827–841.

9. Dearborn R, Kunes S. An axon scaffold induced by retinal axons directs glia to destinations in the *Drosophila* optic lobe *Development*, 2004 131, 2291-2303

10. K.-W Choi, S Benzer Migration of glia along photoreceptor axons in the developing *Drosophila* eye Neuron, 12 (1994), pp. 423–431

11. Rangarajan, R., Q. Gong, and U. Gaul, 1999 Migration and function of glia in the developing Drosophila eye. *Development* 126: 3285–3292.

12. Cafferty P, Auld VJ. No pun intended: future directions in invertebrate glial cell migration studies *Neuron Glia Biol.* 2007 3(1):45-54.

13. Kaplow ME, Korayem AH, Venkatesh TR. Regulation of glia number in Drosophila by Rap/Fzr, an activator of the anaphase-promoting complex, and Loco, an RGS protein. *Genetics.* 2008; 178(4):2003-16.

14. Klämbt C, Glazer L, Shilo BZ. Breathless, a Drosophila FGF receptor homolog, is essential for migration of tracheal and specific midline glial cells. Genes Dev. 1992;6(9):1668-78.

15. Shishido E, Ono N, Kojima T, Saigo K. Requirements of DFR1/Heartless, a mesoderm-specific Drosophila FGF-receptor, for the formation of heart, visceral and somatic muscles, and ensheathing of longitudinal axon tracts in CNS. Development. 1997 Jun;124(11):2119-28.

16. Sutherland D, Samakovlis C, Krasnow MA. branchless encodes a Drosophila FGF homolog that controls tracheal cell migration and the pattern of branching. Cell. 1996 Dec 13;87(6):1091-101.

17. StathopoulosA.,TamB.,RonshaugenM., FraschM. and LevineM. (2004) Pyramus and thisbe: FGF genes that pattern the mesoderm of Drosophila embryos 10.1101/gad.1166404. Genes and Development 18, 687–699.

18. Kadam, S., A. McMahon, P. Tzou, and A. Stathopoulos, 2009 FGF ligands in Drosophila have distinct activities required to support cell migration and differentiation. *Development* 136: 739–747.

19. Franzdottir, S. R., D. Engelen, Y. Yuva-Aydemir, I. Schmidt, A. Aho et al. 2009 Switch in FGF signaling initiates glial differentiation in the Drosophila eye. *Nature* 460: 758–761.

20. Tulin S, Stathopoulos A. Analysis of Thisbe and Pyramus functional domains reveals evidence for cleavage of Drosophila FGFs BMC Dev Biol. 2010;10:83.

21. Madou, M. Fundamentals of Microfabrication; CRC: New York,1997.

22. McDonald, J. C.; Duffy, D. C.; Anderson, J. R.; Chiu, D. T.; Wu, H.; Schueller, O. J. A.; Whitesides, G. M. Fabrication of Microfluidic Systems in Poly(dimethylsiloxane). Electrophoresis 2000, 21, 27-40

23. McDonald JC, Whitesides GM. Poly(dimethylsiloxane) as a material for fabricating microfluidic devices. Acc Chem Res. 2002 Jul;35(7):491-9. Review.

24. Folch, A.; Ayon, A.; Hurtado, O.; Schmidt, M. A.; Toner, M.Molding of Deep Poly(dimethylsiloxane) Microstructures for Microfluidics and Biological Applications. J. Biomech. Eng. 1999,121, 28-34.

25. Li Jeon N, Baskaran H, Dertinger SK, Whitesides GM, Van de Water L, Toner M. Neutrophil chemotaxis in linear and complex gradients of interleukin-8 formed in a microfabricated device. Nat Biotechnol. 2002 Aug;20(8):826-30

26. P.J. Van Haastert, P.N. Devreotes, Chemotaxis: signalling the way forward, Nat. Rev. Mol. Cell Biol. 5 (8) (2004) 626–634.

27. Boyden, S.V. The chemotactic effect of mixtures of antibody and antigen on polymorphonuclear leukocytes. *J. Exp. Med.* 1962 115, 453

28. Corriden R, Insel PA. New insights regarding the regulation of chemotaxis by nucleotides, adenosine, and their receptors. Purinergic Signal. 2012 Apr 15. [Epub ahead of print]

CHAPTER 2: Using the μLane system to estimate the diffusivity of FGF-8

2.1 INTRODUCTION

Fluorescently labeled dextran is a heavily utilized molecule. That is because it is a branched polysaccharide available in a wide range of molecular weights. Because molecular weight is the most significant factor in determining diffusivity[1], dextran is a useful surrogate for modeling transport of non-fluorescent molecules of similar molecular weight. This has been done to validate drug delivery across the blood brain barrier[2], determine the bioavailability of drugs as a function of molecular weight[3], and study the effect of porosity in agarose hydrogels[4].

There are a number of ways to determine the diffusivity of fluorescent molecules. Fluorescent recovery after photobleaching (FRAP) is a reliable method. FRAP involves bleaching a known area, and then tracking how the intensity recovers as new fluorescent molecules diffuse in to fill the gap. Although it's been around for decades[5], the methodology is being continuously improved. For example, the bleach area has been reduced, allowing for FRAP to be used within live cells[6]. Fluorescence Correlation Spectroscopy (FCS) analyzes fluctuations in fluorescence, which physical properties can then be deduced. It can be used to model the transport of intracellular proteins[7-9]. Both FRAP and FCS are used extensively, with much success, but require complex modeling and expensive equipment[10].

This study will use Fick's law of diffusion to predict dextran concentrations, which are then curve fit with experimentally measured intensity values to solve for diffusivity. The method, called Fickian empirical, is simple and robust, and has been used with dextran in hydrogels[11], and silk fibroin films[12]. We will utilize the bridged μLane system, a microfluidic device whose

design and operation has been previously described[13], to collect data. Dextran is frequently used to verify gradient formation in similar devices[14, 15]. Instead of for verification purposes, we will use these curves to find the diffusivity of 20 kDa FITC dextran.

2.2 MATERIALS AND METHODS

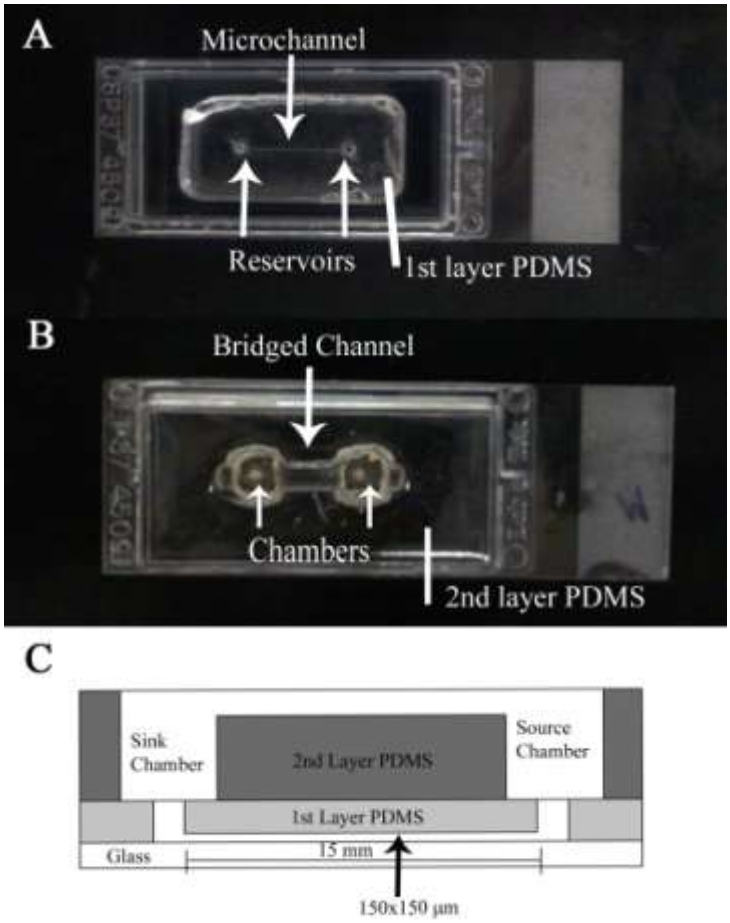

Figure 3: A) 1st layer of PDMS bonded to a glass slide. Two reservoirs are connected by a channel. B) 2nd layer of PDMS bonded to the first layer. A source and sink chamber align on top of the two reservoirs, and a bridge channel connects the two chambers. C) Schematic of the entire system, showing the dimensions of the channel.

2.2.1 µLane System

The bridged µLane is a microfluidic system whose design and operation has been described previously in greater detail[13]. To summarize, it is fabricated from elastomeric molding of two layers PDMS, which are stacked on top of one another, and bonded to a glass slide. The first

layer includes a 150μm diameter by 15mm long microchannel, as well as a source and sink reservoir, which have volumes of 9μL each. The second layer consists of 170μL source and sink chambers, and a small hemispherical bridge channel connecting them. In order to operate, the desired diffusible reagent is placed in the source chamber, and the rest of the system is filled with PBS or media. The bridge channel precisely balances the liquid heights in the source and sink chamber, minimizing the pressure gradient between them and facilitating slow moving flow in the microchannel. This convective-diffusion is what establishes a concentration gradient between the source and the sink reservoir. The gradient can be maintained for several days, and also be modeled computationally and verified experimentally.

2.2.2 Experimental Design

To mimic the microenvironment in which subsequent experiments would utilize cells, μLanes were coated with 50μg/mL Laminin (Sigma-Aldrich, St. Louis, MO) and incubated at 37 C for 1 hour. In 2D coating experiments, the Laminin was then aspirated from the channels. In 3D coating experiments, the now gelled Laminin was left intact. In order to determine bulk flow velocity, 1.9μm fluorescent beads (Duke Scientific, Palo Alto, CA) were injected in the system, and their average velocity was measured. PBS (Mediatech Inc., Herndon, VA) was loaded via a 1mL syringe, until the microchannel, sink reservoir, sink chamber, and bridge channel were full. Then, FITC-Dextran at a concentration of 40μg/mL (20 kDa, Sigma-Aldrich, St. Louis, MO) was added drop wise to the source chamber until it made contact with the PBS in the bridge channel, initiating the system. Fluorescent images of the microchannel were taken every hour for 72 hours at the points x=4mm, x=8mm, and x=12mm, with x=0 being the point where the source reservoir meets the microchannel. Imaging was done using a Nikon TE2000 inverted microscope with a

20x objective and a cooled CCD camera (CoolSNAP EZ, Photometrics, Tucson, AZ) with Nikon software (Nikon Instrument Element 2.30 with 6D module, Morrell Instrument Company Inc., Melville, NY).

2.2.3 Mathematical Modeling and curve fitting

Diffusion in the microchannel was modeled using Fick's law of convective-diffusion:

$$\frac{\partial C}{\partial t} + V\frac{\partial C}{\partial x} = D\frac{\partial^2 C}{\partial x^2} \quad (1)$$

Where C (μg/mL) is concentration, t (s) is time, D (m^2/s) is diffusivity, V (m/s) is velocity, and x (m) is position. This equation was solved using finite-element-analysis in Matlab 7.7 (MathWorks, Natick, MA). The system was modeled as 1D because the length of the channel is significantly larger than the width, making any movement in the y or z direction negligible compared with movement in the x direction. The boundary conditions fixed the source reservoir (x=0) at 40 μg/mL and the sink reservoir (x=15mm) at 0 μg/mL. Initial conditions set the entire length of the channel at 0 μg/mL at t=0. The velocity measured from the beads was used for V. Simulation plots of concentration versus time were compared to experimentally measured plots of fluorescent intensity versus time (intensity being used as an approximation for concentration). Next, a regression was performed that found a D that best fit the simulation. This was done for both 2D and 3D.

In order to compare the results, the Stokes-Einstein equation was solved to estimate D:

$$D = \frac{k_B T}{6\pi\eta r} \quad (2)$$

It is a correlation based on molecular radii that provides a ballpark value of diffusivities, where Kb (m^2kg/s^2K) is Boltzmann's constant, T (K) is temperature, η (kg/m*s) is viscosity, and r is the hydrodynamic radius. An additional equation was required to find r:

(3)

Where r is hydrodynamic radius, and MW is molecular weight. It is a simple, experimentally verified empirical correlation[16].

2.3 RESULTS

By measuring the average displacement of the fluorescent beads over time, a value for bulk velocity was determined, which was then plugged in to equation 1 to generate the plots from figure 2 below. The value was .27 +/- .06 μm/s. That was considered reasonable, because although it was less than previous work doing similar experiments[13], it was within the margin of error. Even though the two values were statistically equivalent, the one from the current study resulted in a steady state time of 2 hours less. This time was also verified experimentally via intensity measurements. Because bulk velocity makes the majority of the contribution to the shape of the plots in figure 2, velocity could be deduced from those plots alone. The fact that velocity values from the plot match the value measured with the bead experiments provides verification that the measured value was accurate. Additionally, the previous experiment used 10 kDa dextran rather than 20, giving the solution a higher density. Given those differences, it would be surprising if the results were the same.

In the 2D experiments, all plots started with a low baseline intensity, which rapidly increased after a few hours. Upon reaching steady state, the intensity remained nearly constant for the duration of the experiment. The steady state time depended on the location within the

channel, with locations closer to the source reaching steady state faster than those further away. The steady state time, defined as reaching 95% of the asymptotic value, was 16 hours.

In the 3D experiment, steady state time was markedly higher at 204 hours. That is because with zero bulk velocity, diffusion dominated transport, which is much slower. Furthermore, instead of peaking at 1 as with 2D, normalized steady state concentrations never reach that high. Instead they peak at lower and lower values the further from the source they are. This difference can be seen noticing the maximum value of the lines in figure 2B. It should be mentioned that 204 hours was beyond the time frame that the device was capable generating reliable data. Beyond about 70 hours, data became erratic and intensities dropped, probably due to reagent evaporation or perhaps bleaching. Even though data were not collected to steady state, enough was recorded to still complete a regression.

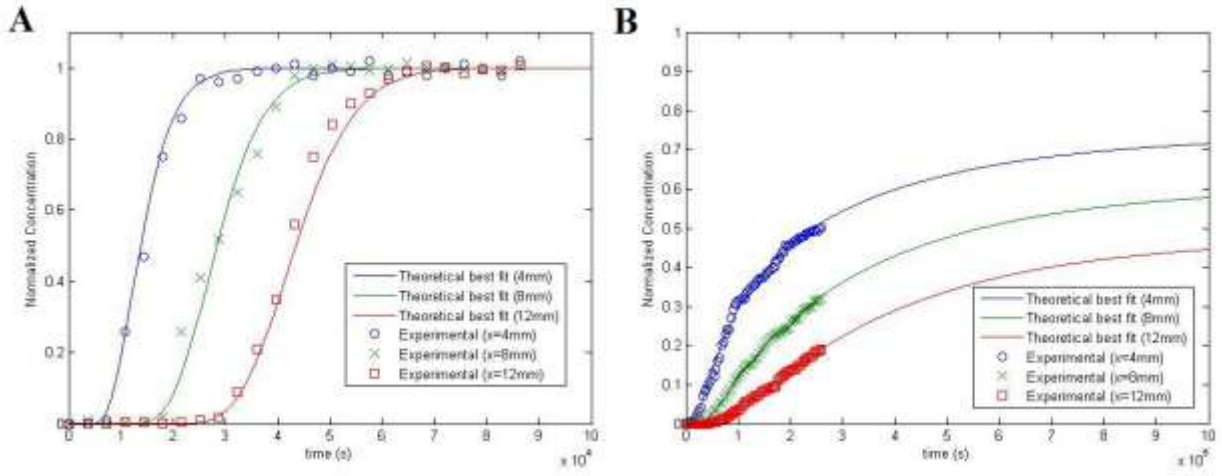

Figure 4: Normalized fluorescent intensity plotted versus time at 4, 8, and 12 mm along with the best fit line. The diffusivity value corresponding with the best fit line is considered to be the free solution diffusivity. Note the x axis is an order of magnitude larger in B than A, indicating the much larger time scale required to reach steady state. A) 2D Laminin coating B) 3D Laminin coating. Results only shown to 72 hours as that is the maximum time that reliable measurements can be made, however, theoretical lines were extended to steady state time.

2.4 DISCUSSION

Diffusivity values from the current study, as well as comparisons from the literature are found in table 1. On the low end at $2.02*10^{-7}$ cm^2/s is the FRAP experiment reported by Brandl et al[11]. That number was lower than their other experiments that used different methods to calculate D. It was suggested that for lower molecular weight dextrans, recovery started occurring during the bleaching phase, which led to an underestimation of D. Interestingly, a different study which also used FRAP to calculate diffusivities of dextran in hydrogels, reported a much higher value[17]. A method exists to correct for recovery during bleaching[10], so perhaps that accounts for the discrepancy.

Table 1: Summary of diffusivity values for both FGF-8 and FITC dextran from the literature as well as the current study.

	D ($*10^{-7}$ cm^2/s)			
Type	FGF-8 (22.5 kDa)	FITC dextran (20 kDa)	Notes	Reference
FCS	5.3		Conjugated to GFP, zebrafish embryo	18
FCS	9.1		Conjugated to Cy5	18
Theoretical	7.7	8.0	Stokes Einstein	
FRAP		2.02	5% hydrogel	11
DOSY		3.04	5% hydrogel	11
Fickian empirical		4.77	5% hydrogel	11
FRAP		4.34	.5% hydrogel	17
Fickian empirical		3.47	silk fibroin film	12
Fickian empirical		6.8	2D, V = .27e-6 m/s	Current Study
Fickian empirical		6.1	3D V = 0 m/s	Current Study

Results from both the 2D and 3D experiments show diffusivities higher than what is reported in the literature. This is to be expected for several reasons. First, FRAP diffusion is a fundamentally different process. It is called self-diffusion, which is diffusion in the absence of a

gradient. Fickian diffusion requires gradients. While the Fickian diffusion coefficients are related to self-diffusion coefficients, they are not the same[19]. Moreover, even studies that used Fickian diffusion coefficients used them in hydrogels or films. The so called "effective diffusivity" is expected to be lower than the free solution diffusivity reported in this study.

FGF-8 was included in the table to test the assumption that a protein of similar molecular weight would have a similar diffusivity. That appears to be true, although it's worth noting that FGF-8 is not fluorescent, and had to be conjugated to GFP or Cy5 for FCS measurements. As such, the entire complex was much heavier than FGF-8 alone, and the values reported should be interpreted as a minimum. Nevertheless, it's possible to use our device to measure diffusivities for a wide range of fluorescent molecules. Those values can then be used to model transport of non-fluorescent substances of similar molecular weight, such as growth factors.

2.5 CONCLUSION

A simple method for measuring the diffusivity of dextran was proposed. It has the advantage of utilizing existing microfluidic devices commonly used for other purposes. While dextran is a heavily studied substance, reported diffusivities typically involved the use of a biomaterial, and free solution diffusivities were unexplored. Our method is easily adaptable to different molecular weights of dextran, and is useful for estimating diffusion coefficients of other molecules such as FGF-8.

REFERENCES

1. Cussler E. *Diffusion: Mass Transfer in Fluid Systems.* Cambridge University Press; Cambridge, UK: 2003.

2. Montenegro L, Trapani A, Latrofa A, Puglisi G. In vitro evaluation on a model of blood brain barrier of idebenone-loaded solid lipid nanoparticles. *J NanosciNanotechnol.* 2012 (1):330-7.

3. Ito Y, Ise A, Sugioka N, Takada K. Molecular weight dependence on bioavailability of FITC-dextran after administration of self-dissolving micropile to rat skin. *Drug Dev Ind Pharm*. 2010 36(7):845-51.

4. Albro MB, Rajan V, Li R, Hung CT, Ateshian GA. Characterization of the Concentration-Dependence of Solute Diffusivity and Partitioning in a Model Dextran-Agarose Transport System. *Cell Mol Bioeng*. 2009 2(3):295-305.

5. Peters, R., J. Peters, K. H. Tews, and W. Bahr. Microfluorimetric study of translational diffusion in erythrocyte-membranes. *Biochim. Biophys. Acta*. 1974. 367:282–294

6. Braeckmans K, Remaut K, Vandenbroucke RE, Lucas B, De Smedt SC, Demeester J. Line FRAP with the confocal laser scanning microscope for diffusion measurements in small regions of 3-D samples. *Biophys J*. 2007 92(6):2172-83.

7. Broderick R, Ramadurai S, Tóth K, Togashi DM, Ryder AG, Langowski J, Nasheuer HP. Cell Cycle-Dependent Mobility of Cdc45 Determined in vivo by Fluorescence CorrelationSpectroscopy. PLoS One. 2012;7(4):e35537.

8. Weidtkamp-Peters S, Weisshart K, Schmiedeberg L, Hemmerich P (2009) Fluorescence correlation spectroscopy to assess the mobility of nuclear proteins. Methods Mol Biol 464: 321–341

9. Wang Z, Shah JV, Berns MW, Cleveland DW (2006) In vivo quantitative studies of dynamic intracellular processes using fluorescence correlation spectroscopy. Biophys J 91: 343–351.

10. Waharte F, Steenkeste K, Briandet R, Fontaine-Aupart MP. Diffusion measurements inside biofilms by image-based fluorescence recovery after photobleaching (FRAP) analysis with a commercial confocal laser scanning microscope. *Appl Environ Microbiol*. 2010, 76(17):5860-9.

11. Brandl F, Kastner F, Gschwind RM, Blunk T, Tessmar J, Göpferich A. Hydrogel-based drug delivery systems: comparison of drug diffusivity and release kinetics. J Control Release. 2010 142(2):221-8.

12. Hines DJ, Kaplan DL. Mechanisms of controlled release from silk fibroin films. *Biomacromolecules.* 2011 14;12(3):804-12.

13. Kong Q, Able RA, Jr., Dudu V, Vazquez M. A microfluidic device to establish concentration gradients using reagent density differences. *Journal of biomechanical engineering* 2010;132:121012.

14. Amadi OC, Steinhauser ML, Nishi Y, Chung S, Kamm RD, McMahon AP, Lee RT. A low resistance microfluidic system for the creation of stable concentration gradients in a defined 3D microenvironment. Biomed Microdevices. 2010 Dec;12(6):1027-41.

15. Kim MJ, Breuer KS. Enhanced diffusion due to motile bacteria. *Physics of Fluids*, 2004 16: L78-L81

16. De Smedt SC, Lauwers A, Demeester J. Structural Information on Hyaluronic Acid Solutions As Studied by Probe Diffusion Experiments. *Macromolecules* 1994, 27, 141-146

17. M.C. Branco, D.J. Pochan, N.J. Wagner, J.P. Schneider, Macromolecular diffusion and release from self-assembled [beta]-hairpin peptide hydrogels, Biomaterials 30(2009) 1339–1347.

18. Yu SR, Burkhardt M, Nowak M, Ries J, Petrásek Z, Scholpp S, Schwille P, Brand M. fgf8 morphogen gradient forms by a source-sink mechanism with freely diffusing molecules. *Nature*. 2009 461(7263):533-6

19. IUPAC. Compendium of Chemical Terminology, 2nd ed. Compiled by A.D. McNaught and A Wilkinson. Blackwell Scientific Publications, Oxford (1997)

CHAPTER 3: FGF-8 Enhances motility of glia in Drosophila

3.1 INTRODUCTION

Glia are important supporting cells in the nervous system. They provide guidance for migrating neurons, as well as wrap and insulate them[1]. They also form the blood brain barrier and even regulate neurotransmitter levels[2]. An important developmental feature is that they must migrate to their final destination. This is typically mediated by scaffold axons which the glia migrate along. That is what happens in the peripheral nervous system during wing formation[3], and the central nervous system in the optic lobe and elsewhere[4-5]. One type of glia, the retinal basal glia, are born in the optic stalk and migrate to R-cells in the eye imaginal disc[6]. Although they require the presence of R-cells to migrate, they do not require axons as a substrate[7]. That was evidence that, most likely, a diffusible signaling molecule was responsible for driving the migration.

FGF signaling has long been known to drive many aspects of development such as differentiation, migration, and tracheal branching[8-9]. Drosophila has two FGF receptors, Branchless and Heartless. These are activated by three ligands: Pyramus, Thisbe, and Breathless. Breathless only binds to Branchless, while Pyramus and Thisbe only bind to Heartless[10]. Use of Heartless was proven in retinal basal glia when it was shown that knocking it out resulted in a reduction of glia number, impaired migration, and lack of differentiation[11].

The purpose of this study is to prove that FGF is in fact a chemoattractant for glia. Previous in vivo work provided circumstantial evidence of this, but an in vitro system capable of mimicking the cellular microenvironment and precisely controlling FGF gradients has never been attempted. In order to isolate and visualize the cells, we utilized the GAL4-UAS system[12] to

drive the expression of GFP in the glia. Repo-Gal4/Tb flies were mated with a UAS-GFP strain. Offspring expressed GFP in glia because Repo (reversed polarity) is a marker specific to glia[13]. Larvae were dissected and their brains dissociated. The cells were then placed in our μLane system[14] and exposed to gradients of FGF-8. Pyramus and Thisbe are FGF-8 homologs[15]. We used FGF-8 because Pyramus and Thisbe are not commercially available. Although they are much larger than FGF-8, the form that is secreted is cleaved, making it of comparable size and presumably similar function[15]. By using the system, we were able to identify FGF as the likely signalling molecule utilized by R-Cells.

3.2 MATERIALS AND METHODS

3.2.1 Fly Stocks

Repo-GAL4/Tb and UAS-GFP stocks were used. They were mated and subsequent F1 offspring were dissected in the 3rd instar larvae stage for use in this study.

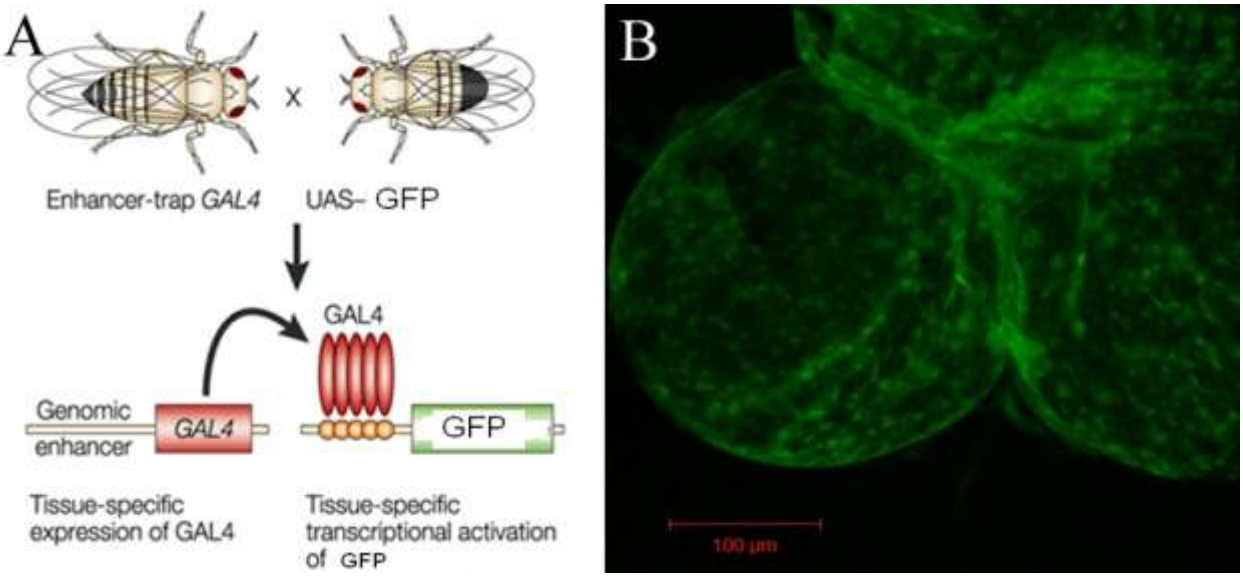

Figure 5: A) Illustration of GAL4-UAS system. Repo-Gal4 flies are mated with UAS-GFP. Offspring express GFP in glia only. B) Confocal image of whole brain, confirming presence of GFP. Scale bar: 100 μm

3.2.2 Confocal Microscopy

Dissected eye brain complex from larvae were cleaned and mounted with Vectashield medium (Vector Laboratories, Burlingame, CA). Images were taken with a Zeiss CLSM-510 (Zeiss, Jena, Germany) and a 40X objective. An argon laser with excitation of 488 nm was used activate the GFP. Images were obtained as Z stacks and processed with LSM software, which converted the Z stacks to a projection.

3.2.3 Cell dissociation and culture

The procedure for culturing glia was adapted from a method established to culture neurons from Drosophila larvae[16]. Third instar larvae were surface sterilized with 70% ethanol. Then they were placed in PBS (Mediatech Inc., Herndon, VA), and their brain complexes were pulled out using forceps. The brains were placed in a solution of .5 mg/mL collagenase (Gibco, Grand Island, NY) in PBS, finely chopped, covered, and incubated at room temperature for 1 hour with slight agitation. The cell suspension was then centrifuged and re-suspended in culture medium consisting of 90% revised Schneider's *Drosophila* medium (Lonza, Walkersville, MD) and 10% heat-inactivated FBS with 50 U/mL penicillin and 50 μg/mL streptomycin sulfate. Cells were incubated at room temperature and atmospheric CO2.

3.2.4 Fluorescent Activated Cell Sorting

FACS was done using a BD FACS Aria II (BD Biosciences, San Jose CA) and FACSDiva 6.1.3 software (BD Biosciences, San Jose CA). The 488 nm laser through a 530/30 filter was used to detect GFP. The 633 nm laser through a 660/20 filter was used to detect To-pro-3 Iodide. 10 μL of To-pro-3 Iodide (Invitrogen, Eugene OR) at 25 μg/mL was added to the sample and incubated 15 minutes.

3.2.5 Experimental Design

The first set of experiments utilized the μLane system described in Chapter 1. Microchannels were coated with 50μg/mL Laminin (Sigma-Aldrich, St. Louis, MO) incubated at 37 C for 1 hour, and then flushed with PBS. Cell solution ($2*10^5$ cells/mL) was loaded via a 1mL syringe, until the microchannel, sink reservoir, sink chamber, and bridge channel were full. Then, FGF-8 (Invitrogen, Frederick, MD) was added drop wise to the source chamber until it made contact with the cell solution in the bridge channel, initiating the system. Concentrations of FGF-8 were 10 ng/mL, 100 ng/mL, and 1000 ng/mL. For the control, media was added instead of FGF-8. After that, images of cells were taken along the length of the channel every hour for 48 hours. Imaging was done using a Nikon TE2000 inverted microscope with a 20x objective and a cooled CCD camera (CoolSNAP EZ, Photometrics, Tucson, AZ) with Nikon software (Nikon Instrument Element 2.30 with 6D module, Morrell Instrument Company Inc., Melville, NY). Experiments were split into two groups: Sorted and unsorted. Sorted cells had been through the FACS, and so they represented a pure population of glia. Unsorted cells came straight from the dissociated brain complex and contained neurons as well as glia.

The second set of experiments used 96 well plates (Corning Inc., Corning, NY) instead of the μLane. Plates were coated with Laminin as described above, and 100 μL of cell solution was added to one well for each experimental condition. FGF-8 was added at a concentration of 1 ng/mL, 10 ng/mL, and 100 ng/mL. For the control, no FGF-8 was added. Experiments were carried out with both sorted and unsorted cells.

3.2.6 Data Analysis and Statistics

Data were analyzed using the Chemotaxis and Migration Tool (Ibidi, Verona, WI) in ImageJ.

Cells were individually tracked using the manual tracking plug-in. Cell trajectories were plotted, along with accumulated distance and motility. In addition, the Chemotactic index was calculated. The chemotactic index is a measure of directed of migration and is defined by equation 1:

$$\mathrm{CI} = \frac{x}{d} \tag{4}$$

Where x is distance toward gradient and d is total accumulated distance. Values approach 1 as cells move more directly toward the gradient, are negative for cells moving away from the gradient, and approach zero in the absence of a gradient. Statistical significance between groups was evaluated using a student's t-test. In the gradient experiments, the Raleigh test was used to assess uniformity of the cell distribution.

3.3 RESULTS

3.3.1 FACS Analysis

FACS data indicated that approximately 5% of the cells were GFP positive, and 59% of all the cells were viable. However, among GFP positive cells, only around 10% were viable. That means that only .5% of the total cell population were GFP positive and viable. As such, only 10,000-20,000 cells were able to be recovered from each sort. The low viability was disappointing, but was somewhat expected due to the collagenase treatment. Glia are apparently more sensitive to collagenase than other cells.

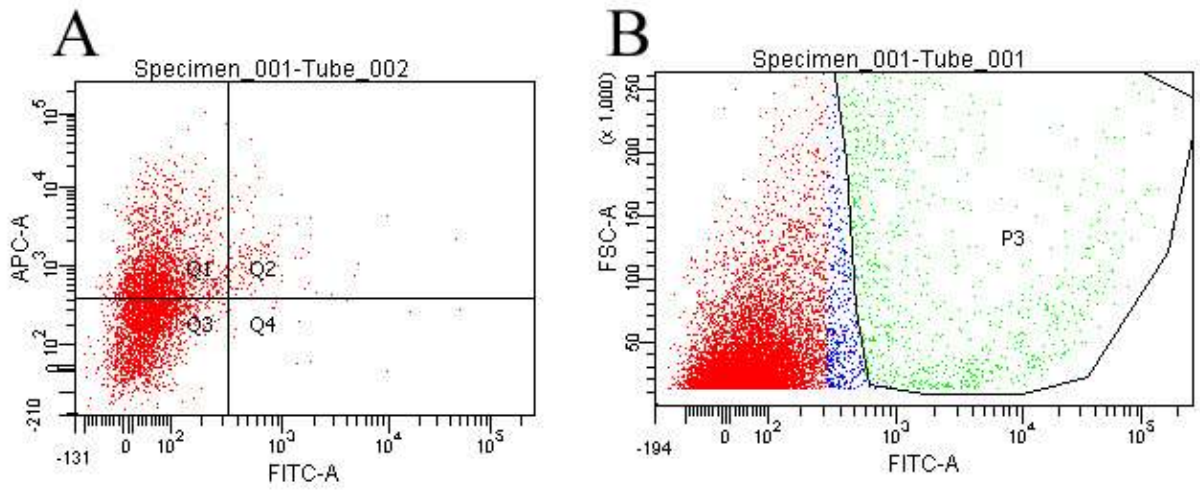

Figure 6: FACS analysis. A) Cells stained with To-pro-3 Iodide as viability marker (APC-A) vs. GFP (FITC-A). Cells in Q3 and Q4 are alive, cells in Q2 and Q4 are GFP positive. Cells in Q4 are both alive and GFP positive. B) Sort is for GFP +/- only. Cells in P3 are GFP+.

3.3.2 µLane experiments

The first set of experiments used the µLane to expose the cells to gradients of FGF-8. When the cells went through the FACS and were sorted, representing a pure glia population, no movement whatsoever could be detected up to 48 hours. Even their morphologies remained constant. The same thing happened for all initial concentrations as well as the control. They couldn't possibly all be dead, because the viability stain in FACS threw all the dead cells out. Of course, the FACS itself could have damaged a certain percentage of them.

Because the cells seemed to be completely inert in isolation, it was decided to add cell solution to the µLane directly after dissociating, and skip the FACS. Results were in marked contrast to the previous experiments. The cells began to move and migrate toward the gradient. The Raleigh test is a statistical test for uniformity of distribution of vectors. Uniform distributions have high P values, while those skewed to one side have lower P values.

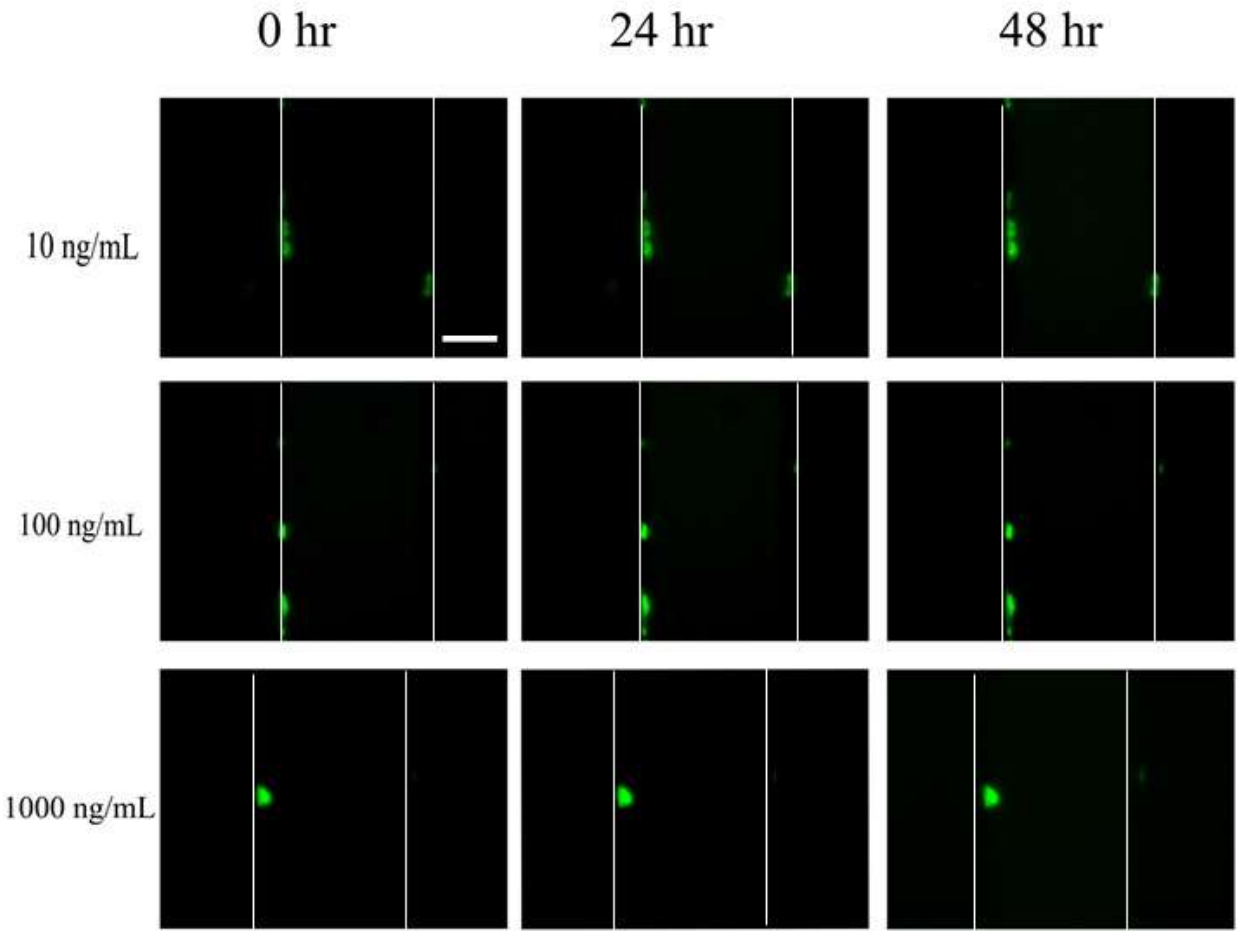

Figure 7: Fluorescent images of glia in the μLane at three time intervals. Concentrations shown are of FGF-8 in the source chamber, concentrations in channels are expected to be a gradient and somewhat lower. Walls of the microchannel are shown in white. After 48 hours, cells showed no signs of migration or morphology changes. Scale bar: 60 μm

Here it was used to quantify the significance of a migration effect. Not surprisingly, the P value was quite high for the control. 1 ng/mL also didn't have a statistically significant cell distribution. 10 ng/mL was highly significant, while 100 ng/mL just barely so. Additionally, the Chemotactic Index was zero, or close to zero for the control and 1 ng/mL. However, it was .25-.36 for 10 ng/mL and 100 ng/mL. That is similar to neutrophils exposed to IL-8 gradients, which

have a CI of .18-.41[17-18] . Although they are a different cell type, they are highly studied and provide a good reference point to compare to other cells. Motility also increased in a statistically significant amount for all concentrations.

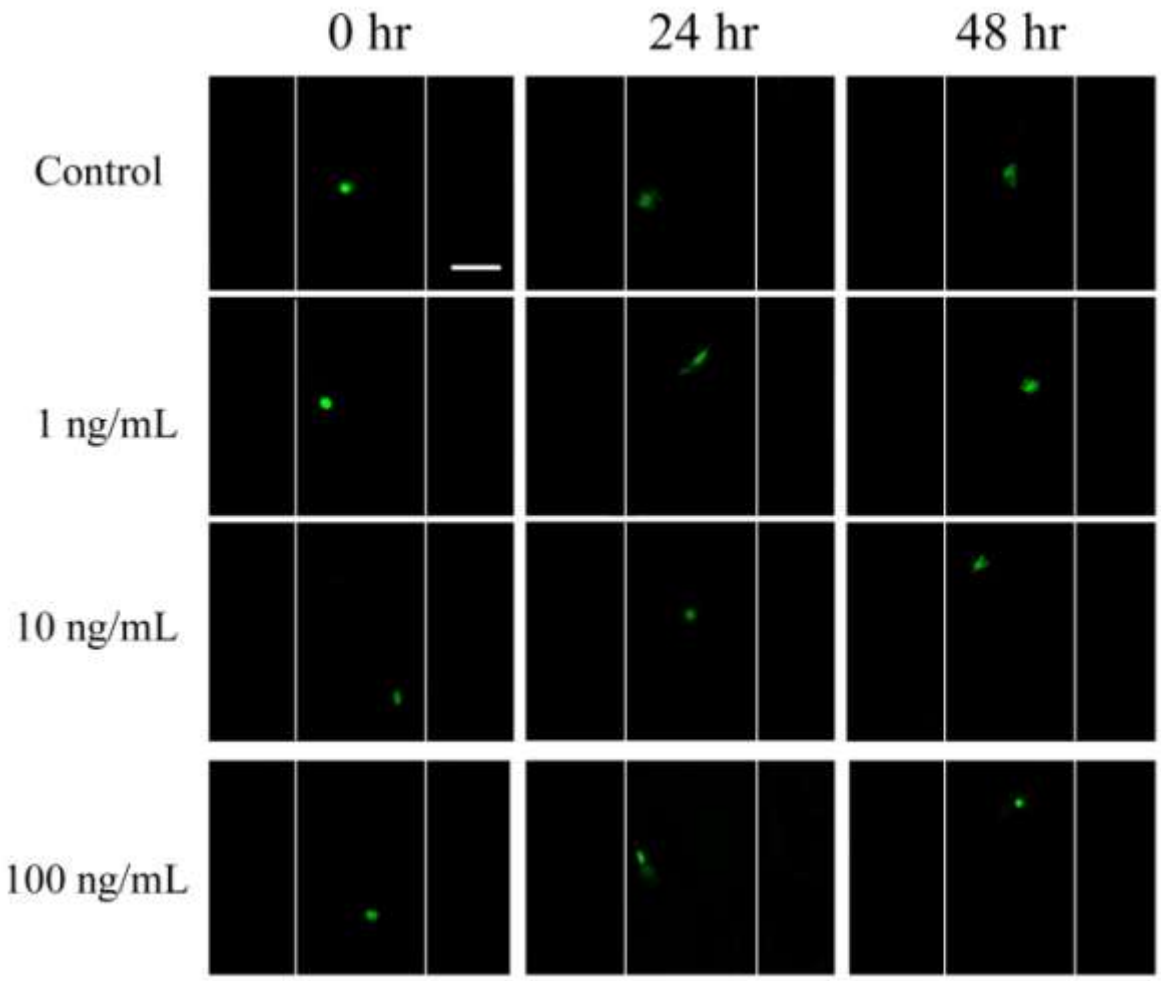

Figure 8: Unsorted cells in the μLane. Concentrations shown are the initial concentrations in the source well, and the gradient is from bottom to top. In the control, cells do not move much from their starting position. With 1 ng/mL movement shows little directional preference. With 10-100 ng/mL there is significant movement toward the gradient. Scale bar: 60 μm

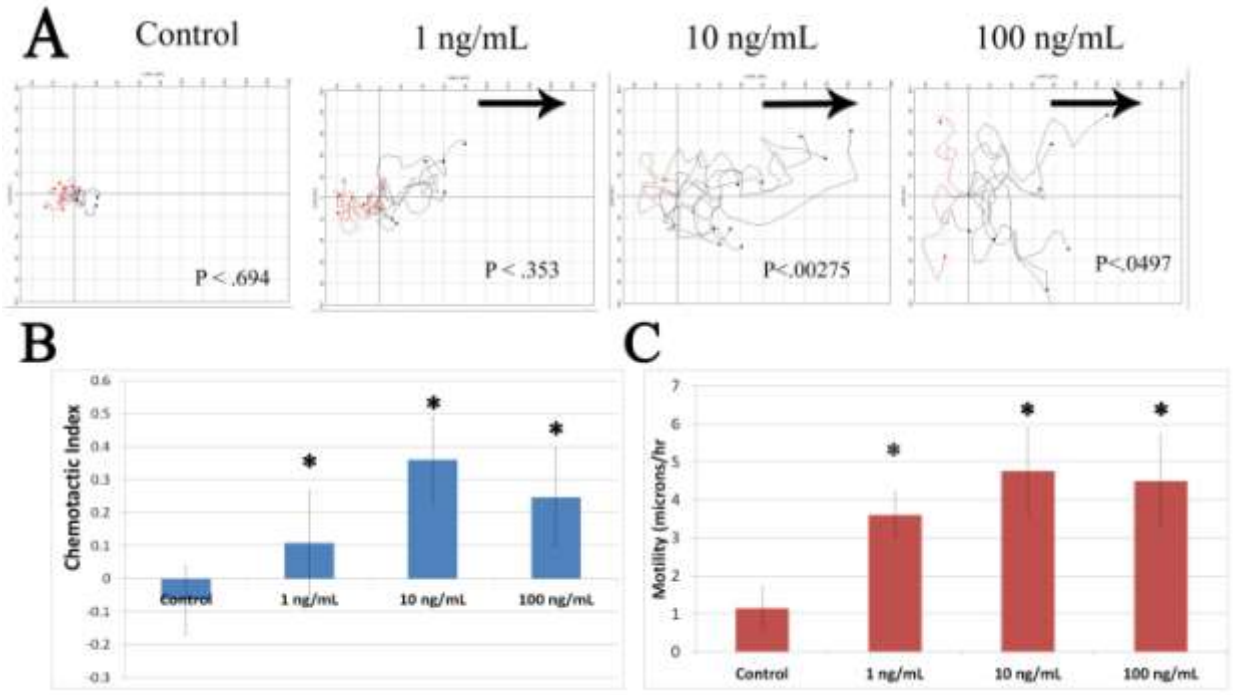

Figure 9: Summary of results of μLane experiments with unsorted cells. A) Plot of cell trajectories normalized to the origin. Each plot contains 10 trajectories with one data point every 2 hours. Gradient is from left to right as indicated by the arrows. P values are for the Raleigh test. Each line on the grid is 20 microns B) Chemotactic index for all experimental conditions. Values reported are means, with error bar (+/-) standard deviation. * indicates P<.05. C) Motility for all experimental conditions.

3.3.3 96 Well Plate Experiments

The next set of experiments examined the cells in wells rather than the microchannel. This was to assess the effect of a uniform concentration of FGF-8 rather than a gradient. When the cells were sorted, there was no statistical difference between the experimental groups and the control. This is similar to what happened with the sorted cells in the μLane experiments, except this time at least there was a small amount of movement. Conversely, the unsorted cells showed a strong increase in both motility and accumulated distance for all experimental conditions.

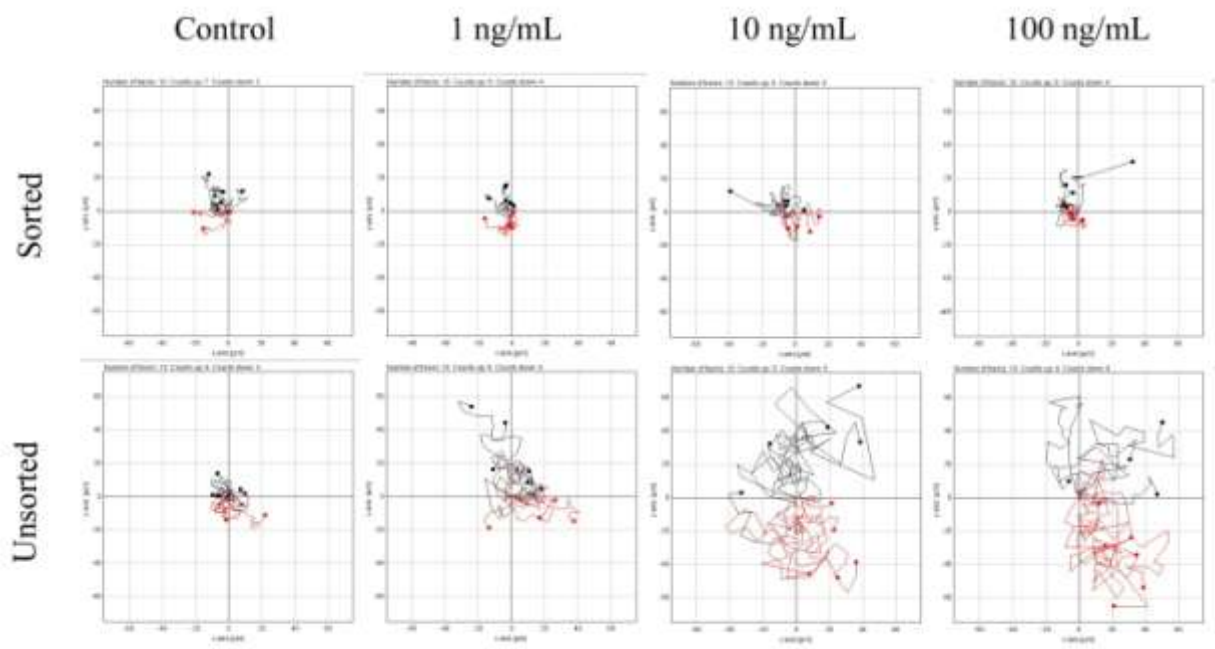

Figure 10: Cell trajectories normalized to the origin for all experimental conditions. Each plot contains 10 paths, and each path contains 1 data point every 2 hours for 48 hours. Concentrations shown are uniform. Note how cells show no directional preference.

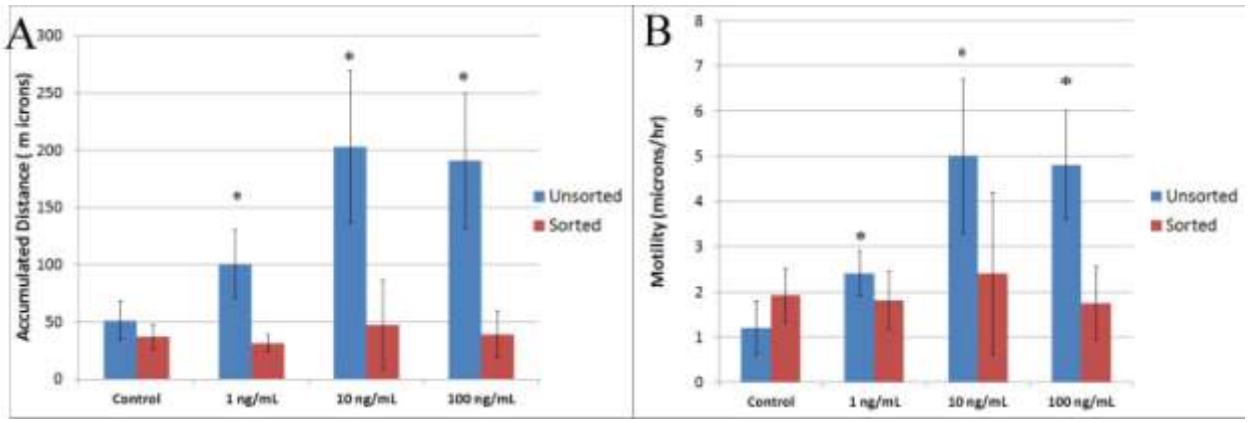

Figure 11: Accumulated distance and motility are plotted for all experimental conditions. Values reported are mean with error bars (+/-) standard deviation. [*] Indicates $p<.05$ compared to the control. Variation is significant for all unsorted concentrations, but not between them. Sorted experiments showed no statistical significance between groups.

3.4 DISCUSSION

There are two ways to interpret the results. The first, is that FACS itself damaged or otherwise rendered the cells immobile. A flow cytometry guide for Drosphila indicated that FACS is harsh on cells and a large percentage of them will be lysed upon return[19]. That could not account for everything though because the sorted cells in the well were clearly alive. Still, FACS probably does have an effect on the cells but it is impossible to isolate. That is because it can't be separated from the effect of other cells. Cells are either pure and have been through FACS or have a mixture of cell types and have not been through FACS.

The other interpretation is that the neurons not only have an effect on the glia, but are required for migration to take place. It is common for glia to migrate along axons[3-5], but retinal basal glia do not require axons as a substrate for migration[7]. However, that doesn't necessarily mean that neurons are not required. Rather than migrating along axons, neurons could secrete diffusible directional cues. Ectopically expressed R-Cells have been shown to attract glia in the absence of an axonal scaffold[7]. Of course, if this diffusible cue was only an FGF-8 like molecule, then our results would have been positive for the sorted cells. The fact that this didn't happen means the situation is more complicated than that, and the literature seems to agree.

Diffusible factors Decapentaplegic (Dpp) and Hedgehog (Hh) have been shown to promote proliferation and motility in retinal basal glia, without specifying direction[20]. The gene Fear of intimacy (Foi) is a regulator of Hh and mutations in it cause glia to overmigrate[21]. Gilgamesh (Gish) also regulates Hh and Gish mutants result in precocious migration[22]. Branchless regulates the temporal onset and extent of migration[23].

Clearly, there are multiple signaling mechanisms that are interdependent and work together produce the desired outcome. We propose that at least one of them such as Dpp, TGF-β

homolog, is secreted by neurons which “activate” the glia. Another signal, presumably Pyr, then provides directional guidance. If that is true, neither Dpp nor FGF’s alone would be sufficient for migration to occur. Rather, they are both required.

3.5 CONCLUSION AND FUTURE WORK

For the first time, an in vitro system was designed and utilized to mimic the microenvironment of glia from Drosophila. Cells were harvested from larvae, dissociated, placed into microchannels, and imaged. FGF-8 was proven to stimulate motility and facilitate migration, but only in the presence of neurons. Future work should generate clones with FGFR knocked out and overexpressed to compare with wild type. This will act as a validation and also determine if receptor expression levels are relevant in determining migratory response. Immunocytochemistry should be done with anti-FGFR antibodies to verify receptor saturation in the presence of FGF. Finally, experiments should be repeated with Dpp to test the hypothesis that it is the missing molecule that works in tandem with FGF ligands to facilitate migration.

REFERENCES

1. Thomas JB, Axon guidance: crossing the midline Curr. Biol., 8 (1998), 102–104

2. Auld VJ, Parker RJ. Roles of glia in the Drosophila nervous system. *Seminars in Cell & Developmental Biology* 17 (2006) 66–77

3. Giangrande A. Glia in the fly wing are clonally related to epithelial cells and use the nerve as a pathway for migration. Development 1994;120:523–34.

4. Dearborn R, Kunes S. An axon scaffold induced by retinal axons directs glia to destinations in the *Drosophila* optic lobe *Development*, 2004 131, 2291-2303

5. Kinrade E., Brates T., Tear G. and Hidalgo A. (2001) Roundabout signaling, cell contact and trophic support confine longitudinal glia and axons in the Drosophila CNS. Development 128, 207–216.

6. K.-W Choi, S Benzer Migration of glia along photoreceptor axons in the developing *Drosophila* eye Neuron, 12 (1994), pp. 423–431

7.Rangarajan, R., Q. Gong, and U. Gaul, 1999 Migration and function of glia in the developing Drosophila eye. *Development* 126: 3285–3292.

8. Shishido E, Ono N, Kojima T, Saigo K. Requirements of DFR1/Heartless, a mesoderm-specific Drosophila FGF-receptor, for the formation of heart, visceral and somatic muscles, and ensheathing of longitudinal axon tracts in CNS. Development. 1997 Jun;124(11):2119-28.

9. Sutherland D, Samakovlis C, Krasnow MA. branchless encodes a Drosophila FGF homolog that controls tracheal cell migration and the pattern of branching. Cell. 1996 Dec 13;87(6):1091-101.

10.StathopoulosA.,TamB.,RonshaugenM., FraschM. and LevineM. (2004) Pyramus and thisbe: FGF genes that pattern the mesoderm of Drosophila embryos 10.1101/gad.1166404. Genes and Development 18, 687–699.

11. Franzdottir, S. R., D. Engelen, Y. Yuva-Aydemir, I. Schmidt, A. Aho et al. 2009 Switch in FGF signaling initiates glial differentiation in the Drosophila eye. *Nature* 460: 758–761.

12. Brand AH, Manoukian AS, Perrimon N. Ectopic expression in *Drosophila*. *Methods Cell Biol.*1994;44:635–54.

13. Xiong WC, Okano H, Patel NH, Blendy JA, Montell C.Repo encodes a glial-specific homeo domain protein required in the Drosophila nervous system.Genes Dev. 1994 Apr 15;8(8):981-94.

14. Kong Q, Able RA, Jr., Dudu V, Vazquez M. A microfluidic device to establish concentration gradients using reagent density differences. *Journal of biomechanical engineering* 2010;132:121012.

15. Tulin S, Stathopoulos A. Analysis of Thisbe and Pyramus functional domains reveals evidence for cleavage of Drosophila FGFs BMC Dev Biol. 2010;10:83.

16. Kim YT, Wu CF. Reduced Growth Cone Motility in Cultured Neurons from Drosophila memory mutants with a defective cAMP cascade. J Neuro, 1996, 16(18):5593

17. Kim D, Lokuta MA, Huttenlocher A, Beebe DJ. Selective and tunable gradient device for cell culture and chemotaxis study. *Lab Chip*. 2009 Jun 21;9(12):1797-800.

18. Lin F, Nguyen CM, Wang SJ, Saadi W, Gross SP, Jeon NL.Effective neutrophil chemotaxis is strongly influenced by mean IL-8 concentration.*Biochem Biophys Res Commun*. 2004 Jun 25;319(2):576-81.

19. de la Cruz AF, Edgar BA. Flow cytometric analysis of Drosophila cells.*Methods Mol Biol*. 2008;420:373-89.

20. Rangarajan R, Courvoisier H, Gaul U.Dpp and Hedgehog mediate neuron glia interactions in Drosophila eye development by promoting the proliferation and motility of subretinal glia. *Mech Dev.* 2001;108(1-2):93-103.

21. Pielage J, Kippert A, Zhu M, Klambt C. The Drosophila transmembrane protein Fear-of-intimacy controls glial cell migration. Dev Biol 2004;275:245–57.

22. Hummel T, Attix S, Gunning D, Zipursky SL.Temporal control of glial cell migration in the Drosophila eye requires gilgamesh, hedgehog, and eye specification genes. *Neuron.* 2002 Jan 17;33(2):193-203.

23. Mukherjee T, Choi I, Banerjee U. Genetic analysis of fibroblast growth factor signaling in the Drosophila eye. *G3 (Bethesda).* 2012 ;2(1):23-8.